Articles

A Symmetry-Driven Search for Electrostatic Interaction Partners in Charybdotoxin and a Voltage-Gated K^+ Channel†

Amir A. Naini and Christopher Miller*

Howard Hughes Medical Institute, Graduate Department of Biochemistry, Brandeis University, Waltham, Massachusetts 02254-9110

Received January 10, 1996; Revised Manuscript Received March 7, 1996⊗

ABSTRACT: A structural model of charybdotoxin bound to a Shaker K^+ channel has emerged from mechanistic and mutagenic analysis of toxin−channel interactions. We test this model by predicting through-space electrostatic interactions between specific pairs of channel−toxin residues. Dissociation constants of channel−toxin variants, determined by radiolabeled toxin binding to *Shaker*-transfected COS membrane fragments, were used to identify pairs of residues located closely enough to interact electrostatically. The results further refine the structural model of the bound complex and produce a more detailed view of the vestibule of the Shaker channel.

Voltage-gated ion channels are essential components of the molecular hardware designed to propagate action potentials in nerve, muscle, and other electrically excitable cells. The voltage-gated K^+ channels terminate the action potential by catalyzing the outward flow of K^+ ions and thereby producing rapid membrane repolarization. The conduction pathways of K^+ channel proteins strongly prefer K^+ over other ions (Hille, 1991), and within the K^+ channel family, the pore-lining "P-region" is the most conserved stretch of amino acid sequence (MacKinnon, 1995). A mechanistic understanding of K^+ permeation will require high-resolution structural information about this part of the channel, information that is currently out of reach for these membrane proteins. For this reason, K^+ channels are being attacked with methods aimed at deducing structural features indirectly. One such approach employs as probes the α-K-toxins (α-KTx),[1] a family of scorpion venom peptides of known structures that specifically bind to K^+ channels in one-to-one stoichiometry and physically block the pore (Miller, 1995). The receptor for these peptides is located on the outer end of the pore and is formed from two noncontiguous stretches of sequence flanking the two ends of the P-region sequence (MacKinnon et al., 1990; Goldstein et al., 1994).

Several groups have been attempting to visualize the structure of the α-KTx receptor, and hence the outer "vestibule" of Shaker-type K^+ channels, by locating pairs of residues, one on channel and one on toxin, that interact locally in the bound complex (Goldstein et al., 1994; Hidalgo & MacKinnon, 1995; Aiyar et al., 1995; Naranjo & Miller, 1996). Considering the toxin as a template for channel structure, these efforts have resulted in a structural model of the toxin complexed with the Shaker K^+ channel (Stampe et al., 1994; Goldstein et al., 1994; Hidalgo & MacKinnon, 1995). Mutational analysis of the full set of solvent-exposed residues of charybdotoxin (α-KTx1.1, abbreviated here as CTX) identified a roughly planar cluster of residues making direct contact with Shaker-type K^+ channels. One of these, K27, interacts with K^+ ions in the channel's conduction pathway. This critical lysine residue is therefore located near the channel's symmetry axis, with the plane of surrounding residues roughly normal to that axis (Goldstein & Miller, 1993).

In this report we build upon a previously identified pair of residues which are close enough in space (4−7 Å) to repel each other weakly via through-space electrostatics: Shaker-427K and CTX-11K (Stocker & Miller, 1994). We seek to examine the hypothesis that these two residues are closely apposed, using a symmetry argument based on the homotetrameric arrangement of voltage-gated K^+ subunits (MacKinnon, 1991; MacKinnon et al., 1993), and, in the process, to discover novel interaction partners. We begin with the proposition that, in the bound complex, CTX-11 lies near one of the four Shaker-427 residues in the tetrameric channel. The three remaining Shaker-427 residues might then be found near other toxin residues, i.e., those projecting at locations equivalent to CTX-11 in 4-fold rotation and at the same altitude above the close contact plane. Since there is good evidence that the channel's symmetry axis is positioned on CTX-K27, we may envision this axis extending up through the body of the bound toxin and thus seek residues about 5−10 Å above the close contact plane and at 90°, 180°, and 270° from CTX-11 as candidates for Shaker-427 interaction partners. Figure 1 introduces the toxin residues that fulfill these criteria for Shaker-427 interaction partners. Using a toxin-binding assay to Shaker channels expressed at high levels in mammalian cell membrane fragments, we confirm the interaction between Shaker-427 and CTX-11 and observe a symmetry-predicted interaction between Shaker-427 (on

† This work was in part supported by NIH Grant GM31768. A.A.N. was supported by NIH Graduate Training Grant 1T32MH19929.

⊗ Abstract published in *Advance ACS Abstracts,* April 15, 1996.

[1] Abbreviations: α-KTx, α-K-toxin; BSA, bovine serum albumin; CTX*, *N*-[1,2-^{3}H]ethylmaleimide-labeled CTX(R19C); EGTA, ethylene glycol bis(β-aminoethyl ether)-*N*,*N*,*N*′,*N*′-tetraacetic acid; HEPES, *N*-(2-hydroxyethyl)piperazine-*N*′-(2-ethanesulfonic acid); MOPS, 3-(*N*-morpholino)propanesulfonic acid; NEM, *N*-ethylmaleimide; Z, pyroglutamate.

S0006-2960(96)00067-0 CCC: $12.00 © 1996 American Chemical Society

an adjacent subunit) and CTX-31. This additional interaction allows us to refine our developing structural picture of CTX docked onto its receptor in the channel's outer vestibule.

MATERIALS AND METHODS

Biochemicals and Reagents. Charybdotoxin variants were expressed in *Escherichia coli* as fusion proteins and purified as described (Park et al., 1991; Stampe et al., 1994). CTX-R19C, prepared and stored as a mixed disulfide with glutathione and reduced before use with DTT, was labeled with *N*-[1,2-^{3}H]ethylmaleimide (40−60 Ci/mmol, New England Nuclear, Boston, MA) as described in detail (Shimony et al., 1994; Sun et al., 1994). This CTX variant, which is radiolabeled at an engineered cysteine exposed on the "back" side of the toxin molecule, far away from the interaction surface, shows binding and blocking characteristics similar to those of unlabeled CTX.

The *Shaker* B K^+ channel variant used has two modifications: an N-terminal deletion of residues 6−46 that removes N-type inactivation (Hoshi et al., 1990) and a point mutation near the P region, F425G, that reveals a high-affinity CTX binding site (Goldstein & Miller, 1992). Mutations of channel and toxin were produced using PCR-mediated mismatch mutagenesis and confirmed by sequencing the PCR-amplified regions.

Transfection of COS Cells and Membrane Preparation. The K^+ channel variants were transiently expressed at high level in COS cells using the mammalian expression plasmid pMT3. Growth and transfection of COS-1 cells and membrane preparation were essentially as described (Oprian et al., 1987; Sun et al., 1994). Briefly, cells were transfected at 50−80% confluency and harvested after 60−65 h by scraping into ice-cold phosphate-buffered saline (PBS), 150 mM NaCl, and 10 mM NaP_i, pH 7.0. All subsequent steps were performed at 4 °C. Cells were pelleted in a clinical centrifuge and resuspended in 150 mM KCl, 2 mM $MgCl_2$, and 5 mM EGTA, pH 10.6, with NH_4OH. Cells were lysed by forcefully passing the resuspension through a 25-gauge needle four times and sonicating with a probe sonicator for 30 s. The lysed cells were centrifuged through a step sucrose gradient (10 mL of sample, 14 mL of 20% w/v sucrose, and 14 mL of 38% w/v sucrose in 20 mM MOPS, pH 7.1) in an SW28.1 rotor for 1 h at 25 000 rpm. The band at the 20−38% sucrose interface was collected, diluted with 3 volumes of cold water, and pelleted for 1 h at 38 000 rpm in a Ti 50.2 rotor. The membrane pellet was resuspended in storage buffer (250 mM sucrose and 10 mM HEPES−KOH, pH 7.3), and aliquots were quickly frozen in dry ice and stored for up to several months at −70 °C.

CTX Binding Assays. (A) Binding of [^{3}H]NEM-CTX (Henceforth Abbreviated CTX) to Transfected COS Membrane Fragments.* Membranes containing 200−300 fmol of receptor sites (equivalent to $\sim^1/_{20}$ of a tissue culture plate's harvest) were incubated at room temperature with varying concentrations of CTX* in 100 μL of binding buffer (150 mM NaCl, 10 mM HEPES−KOH, pH 7.0, and 30 μg/mL BSA) as described (Sun et al., 1994). After a 1-h incubation, membranes were sedimented at 100000*g* for 8 min in an air-driven ultracentrifuge. Supernatants were gently removed, and the unwashed pellets were resuspended with trituration in binding buffer. Both were then dissolved in 10 mL of scintillation fluid and counted to determine free and bound CTX*.

(B) Displacement of CTX by Nonradioactive CTX Variants.* Samples containing 200−500 fmol of receptor sites were incubated as above with 10 nM total CTX* and variable concentrations of unlabeled toxin in 100 μL of binding buffer. Total receptor site concentration was determined by incubating parallel samples with 50 nM CTX*; nonspecific binding was determined by addition of 2000 nM unlabeled CTX. Samples were harvested as above. Samples in which 30−70% of the receptor sites were occupied by CTX* were used to determine the dissociation constant of the unlabeled CTX according to

$$K_{CTX} = \frac{K_{CTX^*}[B^*]}{[CTX^*]}\left(\frac{[CTX]_T - R_T + [B^*]\left(1 + \frac{K_{CTX^*}}{[CTX^*]}\right)}{R_T - [B^*]\left(1 + \frac{K_{CTX^*}}{[CTX^*]}\right)}\right) \quad (1)$$

where K_{CTX^*} is the dissociation constant of CTX* determined from direct binding, [B*] is the receptor-bound CTX* concentration, $[CTX]_T$ is the total unlabeled CTX concentration, and R_T is the total receptor concentration.

Electrostatic Compliance Measurement and Analysis. The electrostatic interaction energy between a specific pair of charged residues, irrespective of other charges on the channel and toxin, can be determined from the Gibbs energies of toxin binding for a set of toxins and channels with charge substitutions made on each (Stocker & Miller, 1994). The electrostatic compliance, σ_{ij}, between two positions, i (on the channel) and j (on the toxin), is defined as

$$\sigma_{ij} \equiv \frac{\partial^2(\ln K_D)}{\partial z_j \partial q_i} \quad (2)$$

where q_i and z_j are the charges at positions on the channel and toxin, respectively. The electrostatic compliance is equal to the electrostatic interaction energy (in kT units) between the two univalent charged residues in question; its value is thus sensitive to the distance, r_{ij}, separating these residues. If a Debye potential is used to approximate the electrostatic energy between two such residues, the electrostatic compliance is directly related to the charge separation:

$$\sigma_{ij} = \frac{F}{RT}\left(\frac{\epsilon e^{-r_{ij}/r_0}}{4\pi\epsilon_0 D r_{ij}}\right) \quad (3)$$

where r_0 represents the Debye length, ϵ is the electronic charge, and D is the dielectric constant. This potential function is only valid for point charges in bulk aqueous solution, and the potential function in the region of the toxin−channel interface will have a more complicated form. However, it is not our intention here to derive absolute distances from electrostatic compliance but rather merely to estimate the relative strengths of electrostatic interactions between chosen residue pairs. The Debye potential function simply allows us to assess the plausibility of our compliance measurements in terms of distances between residues.

RESULTS

In the structural model of the CTX−Shaker complex used to motivate the experiments presented here, CTX-11 lies about 10 Å above the "floor" of the channel vestibule and

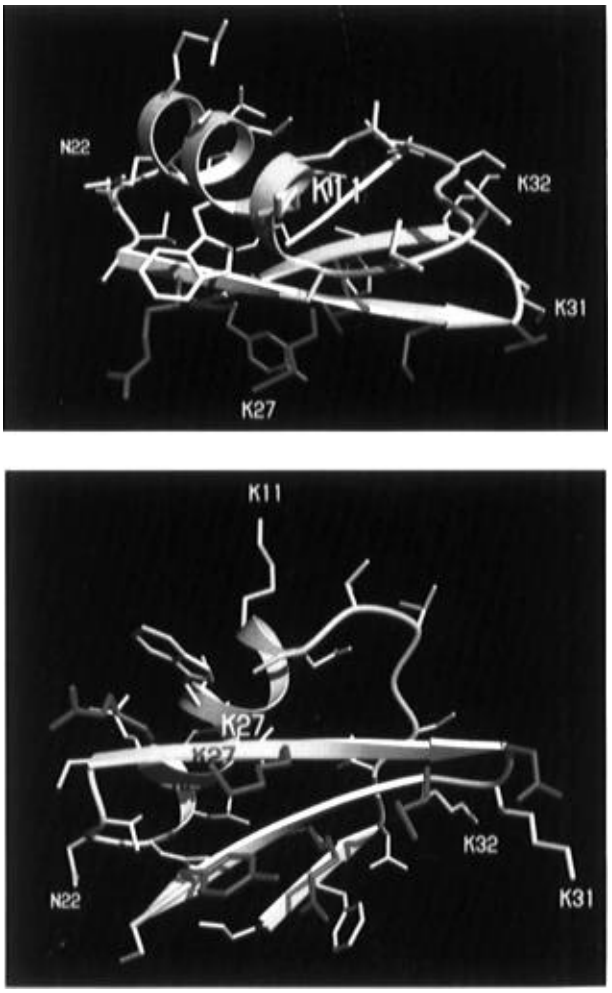

FIGURE 1: Average NMR structure of CTX. Close contact residues are shown in red; residues tested for electrostatic interaction with Shaker-427 are shown in blue; all other solvent-exposed side chains are shown in gray. (A, top) Side view of CTX. K11 projects toward the viewer, N22 projects toward the left, and K31 and K32 project toward the right. (B, bottom) Bottom view of CTX, illustrating the approximately 90° relationship between K11, N22, K31, and K32 about the symmetry axis passing through K27. Images were generated using the Rayscript and Rayshade programs (Kraulis, 1991; Fontano et al., 1996; Kolb, 1996).

projects radially about 15 Å off the central axis that passes through K27, as shown in Figure 1A. In projection view from below, we see (Figure 1B) that two other toxin residues, CTX-31K and CTX-32K, are located at similar distances from the axis, positioned about 90° from CTX-11K. CTX-22N is located 90° in the other direction from CTX-11K. These toxin positions are therefore possible candidates for displaying electrostatic interactions with Shaker-427 of a strength similar to that shown by CTX-11. There are no residues 180° from K11 that fulfill both the altitude and radial projection criteria.

Determination of electrostatic compliance requires many precise determinations of toxin affinities; for a single determination, at the very least a matrix of nine toxin−channel pairs must be examined, and in practice more should be measured (Stocker & Miller, 1994). All previous toxin-mapping experiments have relied upon electrophysiological measurements of toxin inhibition of K^+ channels. Since electrical recording from *Xenopus* oocytes is frequently the most time-consuming procedure in this type of work, we introduce here the use of radiolabeled CTX binding to

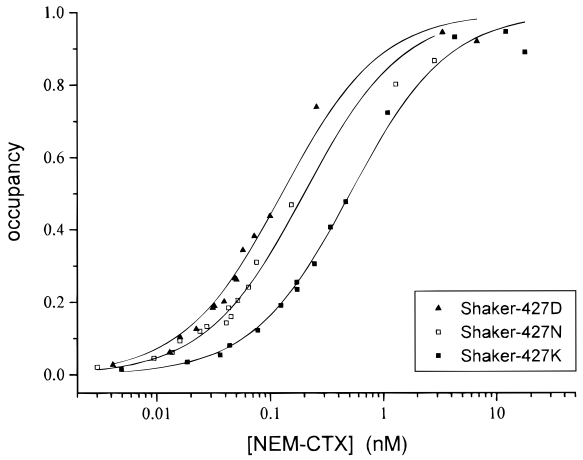

FIGURE 2: Binding of radiolabeled CTX to COS-expressed Shaker channel variants. Equilibrium [^{3}H]NEM-CTX binding to COS cell membranes containing Shaker channels was measured as described in Materials and Methods. Occupancy values were obtained from raw data corrected for the linear nonspecific binding component and normalized to the maximum binding. Receptor concentrations used in these binding experiments were 1.85 nM (Shaker-427D), 2.23 nM (Shaker-427N), and 2.45 nM (Shaker-427K). Nonspecific binding was always <10% of total binding at the highest toxin concentration used. Curves are drawn according to a Langmuir isotherm with the following K_D values: 0.12 nM (Shaker-427D); 0.20 nM (Shaker-427N); 0.50 nM (Shaker-427K).

transfected COS cell membranes to measure toxin dissociation constants. This system has been used for high-level expression of functional Shaker channels and is well characterized (Sun et al., 1994). Equilibrium binding curves of CTX* to COS-expressed Shaker channels fit Langmuir isotherms well, indicating homogeneous channel populations (Figure 2). As shown previously with electrophysiological assay in *Xenopus* oocytes (Stocker & Miller, 1994), toxin affinity decreases as the charge at Shaker-427 varies from negative to neutral to positive. The standard-state Gibbs energy of toxin binding increases approximately linearly with charge at Shaker-427, increasing 1.8 kJ/mol per unit charge. This linear variation is consistent with a through-space electrostatic interaction between this channel residue and the bound toxin, as previously characterized and discussed in detail (Stocker & Miller, 1994). The destabilization of toxin binding by positive charge at Shaker-427 shows that the electrostatic potential experienced at Shaker-427 changes by approximately +5 mV upon toxin binding; this result is reasonable, since CTX* carries a net charge of about +4. This potential is substantially less than the value determined on the same channel expressed in *Xenopus* oocytes; at least part of this difference appears to be due to glycosylation differences in the two expression systems (data not shown) and is currently under investigation.

Our purpose here is to determine the electrostatic interaction of charged residues at Shaker-427 with *particular* residues on CTX. The electrostatic compliance value can be used as a diagnostic tool toward this purpose. Figure 3A illustrates the principle for Shaker-427 and CTX-11. We measure toxin binding as a function of charge at Shaker-427, reporting free energy values for unlabeled CTX, measured by displacement of labeled CTX*. Wild-type toxin carries a positive charge at position 11 (CTX-11K), and affinity varies with q_{427} quantitatively as it does for labeled CTX*. This shows that the potential change induced by toxin binding at Shaker-427 is not affected by NEM

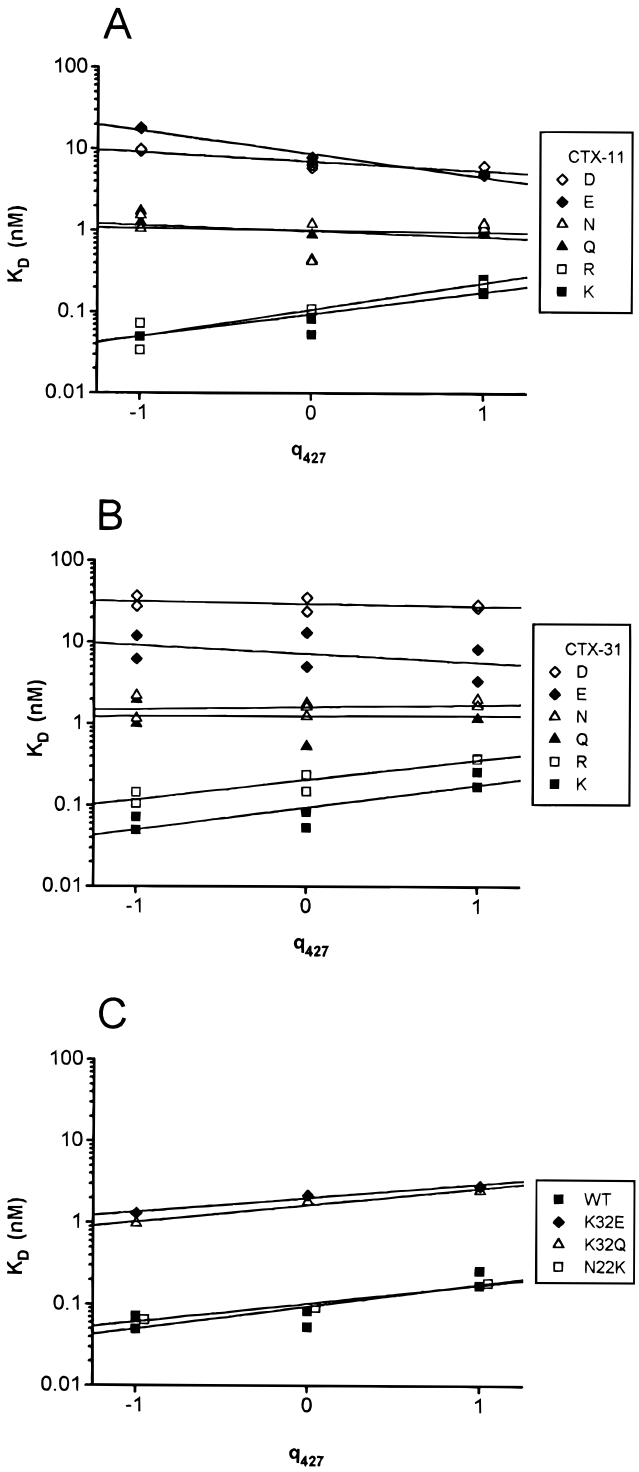

FIGURE 3: Dependence of toxin binding on charge at Shaker-427 and CTX-11, -22, -31, and -32. Dissociation constants of unlabeled toxin binding to Shaker-427 variants were measured using displacement of labeled toxin binding, as described in Materials and Methods. Dependence of binding on charge was determined using the least-squares slope for each toxin variant on six channel variants (Shaker-427K,R,N,Q,E,D). (A) Charge altered at CTX-11. (B) Charge altered at CTX-31. (C) Charge altered at CTX-22 and -32. The points for CTX-22 are shifted 0.05 charge unit for visibility. Dissociation constants for these toxin mutants were determined using Shaker-427K,N,D. For CTX-22, only one toxin charge mutant was tested.

modification of CTX, even though this toxin variant (synthesized from CTX-R19C) carries one less positive charge than does wild-type toxin. In contrast, when the charge at CTX-11 is changed, the slope of the ΔG *vs* q_{427} curve

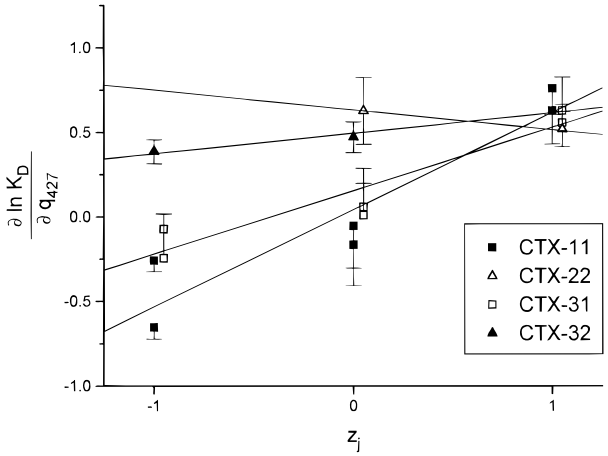

FIGURE 4: Electrostatic compliance for Shaker-427 and selected CTX positions. Least-squares slopes from Figure 3 are plotted versus charge at toxin positions 11, 31, and 32. For clarity, the points for CTX-31 and CTX-22 are shifted 0.05 charge unit, and some error bars are displayed in only one direction. Electrostatic compliance values, measured from least-squares slopes on this plot, are reported as slope ± SD: $\sigma_{427,11} = 0.57 \pm 0.10$, $\sigma_{427,31} = 0.38 \pm 0.06$, $\sigma_{427,32} = 0.16 \pm 0.05$, and $\sigma_{427,22} = -0.11$.

progressively decreases. This slope (and hence the potential induced by toxin binding at Shaker-427) is close to zero for uncharged toxin mutations (CTX-11Q,N), and it actually reverses sign for negatively charged mutations (CTX-11D,E). This inversion of slope for the negative mutations is impressive: whereas these toxins have net charge of +3, they are perceived by Shaker-427 as negatively charged molecules. Thus, the charge at CTX-11 dominates the electrostatic interaction of the toxin with Shaker-427, indicating the proximity of these residues in the toxin−channel complex. The energy of electrostatic interaction is obtained by plotting the slopes of the linear regressions from Figure 3A versus charge at CTX-11, a compliance plot (Figure 4). The slope of the compliance plot is then a quantitative measure of the strength of interaction between the two chosen residues. The electrostatic compliance calculated from these data ($\sigma_{427,11} = 0.57 \pm 0.10$) is close to that previously determined (Stocker & Miller, 1994) on oocyte-expressed channels (0.85 ± 0.15).

Having confirmed that the toxin binding assay agrees with previous electrophysiological results, we now ask about Shaker-427 interactions with the three other toxin residues located in approximately 4-fold equivalent positions: CTX-22, CTX-31, and CTX-32. Of these three positions, only CTX-31 produces an interaction with Shaker-427. As seen with CTX-11 above, the slope of the ΔG *vs* q_{427} curve progressively decreases as charge at CTX-31 is neutralized and then made negative (Figure 3B). This slope variation is not observed in the ΔG *vs* q_{427} curves for CTX-22 and CTX-32 charge mutants (Figure 3C). As before, the electrostatic compliance can be determined by plotting the slopes of the ΔG *vs* q_{427} curves versus toxin residue charge at these positions (Figure 4). The electrostatic compliance for CTX-31 ($\sigma_{427,31} = 0.38 \pm 0.06$) is significantly smaller than that seen with CTX-11. Thus, in the bound complex, CTX-31 lies slightly farther away from Shaker-427 than does CTX-11 but considerably closer than CTX-22 or -32.

To transform values of electrostatic compliance into absolute distance requires knowledge of the distance dependence of the electrostatic potential arising from a source

charge on the protein's aqueous surface. To make such absolute distance estimates thus requires either qualified caution or unqualified foolhardiness, and we will continue to favor the former attitude. We have argued tentatively (Stocker & Miller, 1994) that the CTX-11/Shaker-427 distance is about 5 Å. Whatever the merits of this argument, the CTX-31/Shaker-427 distance should be similar. The validity of this distance estimate is further suggested by our results placing K32 far away, electrostatically speaking, from Shaker-427. The amino groups of K31 and K32 are separated by only 8−10 Å on the CTX molecular surface, which places K32 about 10−12 Å from Shaker-427. Therefore, the potential must fall to near zero at this distance.

DISCUSSION

To draw structural conclusions about membrane proteins from purely functional measurements is a highly uncertain venture. We are thus compelled to tread carefully when attempting to envision the shape of the CTX receptor at the external end of the Shaker pore from the known structure of CTX. However, an accumulating body of evidence over the past few years gives us confidence that the fundamental assumptions of the toxin-mapping approach are valid: that the α-K-toxins physically occlude the pore (MacKinnon & Miller, 1988; Giangiacomo et al., 1992; Goldstein & Miller, 1993), that voltage-gated K^+ channels are 4-fold symmetric (MacKinnon, 1991, 1993), that the toxin backbone's solution structure is sufficiently rigid to provide a known template for its structure on its receptor site (Bontems et al., 1991, 1992; Krezel et al., 1995), that toxin point mutants exert their functional effects locally (Stampe et al., 1994), and, most importantly, that residue K27 of bound toxin is located close to the channel's axis of 4-fold symmetry (Park & Miller, 1992; Goldstein & Miller, 1993; Ranganathan et al., 1996). These assumptions, along with the experimentally measured energetics of toxin binding, have led to a model of bound toxin that serves as a starting point for deducing the surface topography of the vestibule of K^+ channels.

Specifically, using the average NMR-determined solution structures of homologous toxins, three groups have converged to roughly similar views of the orientation of toxin on its receptor (Goldstein et al., 1994; Hidalgo & MacKinnon, 1995; Aiyar et al., 1995). The common feature of this canonical model is a relatively flat surface formed by the five to six toxin residues making close contact with the channel; this surface is oriented normal to the channel's symmetry axis. In our model based on the average CTX structure, the orientation of toxin on its receptor is defined by three roughly orthogonal axes emanating from C_α of K27 (Figure 1A). The *z*-axis, which lies along the assumed channel axis, passes through the body of the toxin through C_α of C13; the *x*-axis extends in the positive direction through C_α of M29 and in the negative through C_α of R25; finally, the *y*-axis extends into the plane of the figure through C_α of Z1.

In this report we seek to expand upon the observation (Stocker & Miller, 1994) that CTX-11K is located near enough to Shaker-427K for these two residues to interact electrostatically. Our structural model of bound CTX demands that Shaker-427 (in opposite or adjacent subunits) must also interact electrostatically with any CTX residues found at locations equivalent to K11 in 4-fold symmetry, i.e., about 5−10 Å above K27, and extending 15 Å in radius off the *z*-axis at angles of ±90° or 180° from K11. There are three possible candidates for such equivalent positions (Figure 1B): K31 or K32, located at roughly at 90° rotation, and N22, at a 270° rotation, from K11. Of these three residues, only K31 exhibits electrostatic interaction with Shaker-427, with an electrostatic compliance value only slightly less than that given by CTX-11 itself.

We were initially surprised by the failure of CTX-32 to act as an electrostatic equivalent of CTX-11. Our original model of the complex, which is based on the CTX average NMR structure, places K32 closer than K31 to a position equivalent to K11. In this orientation of toxin, K31 is situated at a low elevation off the floor of the vestibule, near the cluster of residues that directly contact the channel; at such a position, K31 would not be expected to interact with the same residue as does K11, which is elevated about 10 Å above the floor. Our experimental results force us to refine this picture. The measured electrostatic compliance values identify K31 as a near equivalent to K11, and they tell us that K32 is located far away from any of the four Shaker-427 residues in the complex. Despite the many structural unknowns in the system, this conclusion is solid, since all residues involved are solvent-exposed and since the mechanism of interaction—through-space electrostatics—is nonspecific and well understood.

Is it possible to modify our original orientation of CTX on its receptor to accommodate these two new constraints regarding the relative positions of K11, K31, and K32? It turns out that if we consider only the average structure of CTX as a rigid body, there is no plausible way to do this and at the same time maintain the central position of K27 and the topographical constraints demanded by the channel's 4-fold symmetry (Stampe et al., 1994). However, if we examine the range of allowed side-chain configurations, the problem is easily solved. Figure 5A illustrates the mobilities of the pertinent side chains by displaying 12 overlain energy-minimized structures of CTX (Bontems et al., 1992). The view of CTX shown in this figure was obtained by tilting the toxin 20° about the *x*-axis, bringing K11 forward and down, and 10° about the *y*-axis, moving K31 (and K32) upward. In this orientation, residues K11 and K31 move into roughly equivalent positions, about 5 Å above the floor at K27, and K32 is positioned at a higher altitude than in the initial model, farther away from Shaker-427. These tilts place N22 at about the same altitude as K32 and therefore far from Shaker-427.

Adjusting the toxin's orientation in this way subtlely changes our view of the close interaction surface. The reorientation process moves R25 downward toward the channel surface and lifts M29 and N30 up and away from the postulated flat floor. This movement would be disallowed by considerations of symmetry in the rigid average structure (Stampe et al., 1994); since R25 and M29 are at nearly equivalent positions on opposite sides of the symmetry axis through K27, they should be at equivalent heights. However, the individual minimized structures show ample flexibility in the R25 side chain, and they display several configurations in which this symmetry constraint is readily satisfied. This reorientation also lifts R34 and Y36 slightly with respect to their positions deduced from the average structure. We do not imagine that the side-chain configurations observed in the *solution* structures of CTX accurately

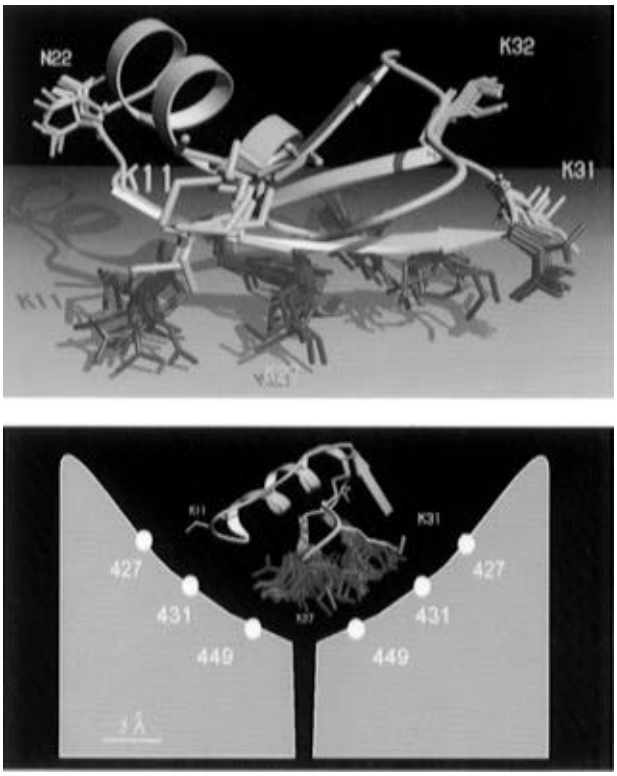

FIGURE 5: Individual energy-minimized structures of CTX with overlain residues. (A, top) Side view of CTX with close contact residues in red and K11, N22, K31, and K32 in blue, showing the refinement tilting the toxin down at K11 and up at K31. These tilts place K11 and K31 at approximately the same altitude and leave N22 and K32 significantly higher. Note the flexibility of R25 (left of K27) away from the close contact plane. (B, bottom) Side view of CTX docked onto an outline representing the channel's outer vestibule. Overlain close contact residues are shown. For clarity, side chains from only one model are shown for K11, K31, K32, and N22. A cross section of two diagonally opposed channel subunits is displayed, with white circles indicating the approximate positions of Shaker-427, -431, and -449. The channel vestibule forms a shallow bowl, extending from the pore at a slight pitch to a distance of approximately 15 Å.

represent the configurations of toxin bound to its receptor; these must certainly adjust to achieve complementarity and favorable energetics in the toxin−channel complex. Instead, we have used the collection of energy-minimized CTX structures to examine side-chain flexibilites and identify configurations that could plausibly exist in the bound complex, while retaining harmony with the electrostatic measurements and the 4-fold symmetry of the Shaker channel.

The topographical picture of the channel vestibule emerging from this refinement is one of a shallow bowl with sides rising at a shallow angle from the pore to a distance of at least 15 Å from the central axis (Figure 5B). The view of the bowl from above is not circular but rather pinwheel-shaped (Goldstein et al., 1994), and the toxin sits with the shallow arc defined by R25-K27-M29-N30 aligned with the long axis of the pinwheel. This refined orientation of CTX also maintains harmony with the picture that has been developing recently, as several laboratories have sought interacting pairs of residues between Kv1-type channels and α-K-toxins. In particular, the positions of CTX-11 and CTX-31 studied here place Shaker-427 at 15−20 Å radius from the external pore opening; this is consistent with the location of Shaker-431, deduced from close interactions with R24 and R31 in α-KTx3.2, a CTX homologue, at a radius of 12−15 Å from the central axis (Hidalgo & MacKinnon, 1995). The close contact surface on α-KTx3.2 has a conical shape, in contrast to the flat surface in CTX, so the sloped topography of the receptor deduced using this homologue is similar to our refined model (Ranganthan et al., 1996). The new position of M29 continues to place its interaction partner, Shaker-449 (Naranjo & Miller, 1996), which can form a binding site for tetraethylammonium (Heginbotham & MacKinnon, 1992), at about 5 Å from the channel axis; in a *Shaker* homologue, this position was inferred to interact with CTX-R25 (Aiyar et al., 1995), a result that makes sense because of the equivalence, in 4-fold rotation about K27, of CTX-R25 and CTX-M29.

The channel residue under study here, Shaker-427, lies in linear sequence near the beginning of the major CTX−receptor determinants (Miller, 1995), just on the N-terminal side of the P-region loop, which contributes directly to the K^+ conduction pore (MacKinnon, 1995). Recent experiments applying cysteine-substitution mutagenesis to voltage-gated K^+ channels reveal that 13 continuous residues (427−439 in the Shaker sequence) appear, from their pattern of reactivity to thiol regeants, to project side chains into aqueous medium from one side of an α-helix (Lü & Miller, 1995; Gross & MacKinnon, 1996). This putative four-turn helix would begin in the wide CTX receptor near Shaker-427 and run inward at a slight pitch toward the channel's symmetry axis. Indeed, the proposed helix terminates in the narrow pore region, at a residue, Shaker-439, that has been suggested (Lü & Miller, 1995) to contribute physically to the "gate" occluding the pore in the channel's closed conformation. Thus, the toxin-based approach offered here, in combination with other functional probes of K^+ channels, is uncovering increasingly detailed structural features of these membrane proteins, characteristics of surface topography and secondary structure which ultimately underlie their biological functions.[2]

ACKNOWLEDGMENT

We are grateful to L. Heginbotham and D. Naranjo for helpful criticisms and to C. Williams for technical assistance.

REFERENCES

Aiyar, J., Withka, J. M., Rizzi, J. P., Singleton, D. H., Andrews, G. C., Lin, W., Boyd, J., Hanson, D. C., Simon, M., Dethlefs, B., Lee, C., Hall, J. E., Gutman, G. A., & Chandy, K. G. (1995) *Neuron 15*, 1169−1181.

Bontems, F., Roumestand, C., Gilquin, B., Menez, A., & Toma, F. (1991) *Science 254*, 1521−1523.

Bontems, F., Gilquin, B., Roumestand, C., Menez, A., & Toma, F. (1992) *Biochemistry 31*, 7756−7764.

Fontano, E., Peisach, D., & Peisach, D. (1996) *Rayscript* (see http://www.sb.fsu.edu/~fontano/rayscript.html for more information and program download).

Giangiacomo, K. M., Garcia, M. L., & McManus, O. B. (1992) *Biochemistry 31*, 6719−6727.

Goldstein, S. A. N., & Miller, C. (1992) *Biophys. J. 62*, 5−7.

Goldstein, S. A. N., & Miller, C. (1993) *Biophys. J. 65*, 1613−1619.

Goldstein, S. A. N., Pheasant, D. J., & Miller, C. (1994) *Neuron 12*, 1377−1388.

Gross, A., & MacKinnon, R. (1996) *Neuron* (in press).

[2] Figures, coordinates, and additional information on the results presented are available from http://www.ccs.brandeis.edu/~naini/ctx.html.

Heginbotham, L., & MacKinnon, R. (1992) *Neuron 8*, 483−491.
Hidalgo, P., & MacKinnon, R. (1995) *Science 268*, 307−310.
Hille, B. (1991) *Ionic Channels of Excitable Membranes*, 2nd ed., Sinauer Associates, Sunderland, MA.
Hoshi, T., Zagotta, W. N., & Aldrich, R. W. (1990) *Science 250*, 533−538.
Kolb, C. (1996) *Rayshade* (see http://www-graphics.stanford.edu:80/∼cek/rayshade/ for more information and program download).
Kraulis, P. (1991) *J. Appl. Crystallogr. 24*, 946−950.
Krezel, A. M., Kasibhatla, C., Hidalgo, P., MacKinnon, R., & Wagner, G. (1995) *Protein Sci. 4*, 1478−1489.
Lü, Q., & Miller, C. (1995) *Science 268*, 304−307.
MacKinnon, R. (1991) *Nature (London) 500*, 232−235.
MacKinnon, R. (1995) *Neuron 14*, 889−892.
MacKinnon, R., & Miller, C. (1988) *J. Gen. Physiol. 91*, 335−349.
MacKinnon, R., Heginbotham, L., & Abramson, T. (1990) *Neuron 5*, 767−771.
MacKinnon, R., Aldrich, R. W., & Lee, A. W. (1993) *Science 262*, 757−759.
Miller, C. (1995) *Neuron 15*, 5−10.
Naranjo, D., & Miller, C. (1996) *Neuron 16*, 123−130.
Oprian, D. D., Molday, R. S., Kaufman, R. J., & Khorana, H. G. (1987) *Proc. Natl. Acad. Sci. U.S.A. 84*, 8874−8878.
Park, C. S., & Miller, C. (1992) *Neuron 9*, 307−313.
Park, C. S., Hausdorff, S. F., & Miller, C. (1991) *Proc. Natl. Acad. Sci. U.S.A. 88*, 2046−2050.
Ranganthan, R., Lewis, J. H., & MacKinnon, R. (1996) *Neuron 16*, 131−139.
Shimony, E., Sun, T., Kolmakova-Partensky, L., & Miller, C. (1994) *Protein Eng. 7*, 503−507.
Stampe, P., Kolmakova-Partensky, L., & Miller, C. (1994) *Biochemistry 33*, 443−450.
Stocker, M., & Miller, C. (1994) *Proc. Natl. Acad. Sci. U.S.A. 91*, 9509−9513.
Sun, T., Naini, A. A., & Miller, C. (1994) *Biochemistry 33*, 9992−9999.

BI960067S